A Study of Harmonic Distortion Limit Change During the Reconfiguration Process of the Smart Grid

by

Wenyue Yang

A dissertation submitted to the Graduate Faculty of
Auburn University
in partial fulfillment of the
requirements for the Degree of
Master of Science

Auburn, Alabama
August 2nd, 2014

Smart grid, harmonic distortion limit,
reconfiguration,

Approved by

Mark Halpin, Chair, Professor of Power System
John Hung, Professor of State-Variable Analysis of Systems
Bogdan Wilamowski, Professor of Analog Circuit Design

Abstract

On the purpose to find out if harmonic distortion limits of customer installations will change during a smart grid reconfiguration process, the thesis was completed. The smart grid concept has been widely accepted to gradually improve the current power system which can be made more efficient, reliable, and secure. However, reconfiguration, which will happen frequently in a smart grid concept, may bring appreciable changes to harmonic distortion limits of customer installations. This phenomenon may be an issue of concern in the smart grid concept. In this thesis, a 30-bus power system will be used as the test system, MATLAB codes about the calculation of short-circuit current will be written, and harmonic limit results will be collected, presented, and analyzed. A conclusion will be drawn that the reconfiguration process of a smart gird could apparently change harmonic limits of some of the customer installations. Short-circuit ratios of several load buses in the test system will be studied in detail to obtain the pattern of harmonic limit value distribution in all the load buses; histograms will be made to clearly explain the pattern.

Acknowledgments

This thesis could not have been finished without the support from my advisor, my parents, my classmates and my friends. First and foremost, I am deeply and sincerely grateful to my advisor Mark Halpin, distinguished professor of Alabama Power, who provided me with patient guidance, insightful suggestions and constant encouragement. I am also very grateful to my parents, who gave me love, encouragement and financial support. In addition, I appreciate the help from my classmates and friend, who answered my questions and helped me with MATLBA code problems.

Table of Contents

List of Tables

List of Figures

List of Abbreviations

AMI	Advanced Measure Infrastructure
CIN/SI	Complex Interactive Networks/System Initiative
EPRI	Electric Power Research Institute
FERC	Federal Energy Regulatory Commission
FLISR	Fault Location Isolation and Service Restoration
HEMS	Home Energy Management Systems
MLC	Maximum Load Current
PPC	Point of Common Coupling
SCR	Short-Circuit Ratio
SLG	Smart Load Management
SSC	Short-Circuit Current
TDD	Total Demand Distortion
THD	Total Harmonic Distortion
USDoE	United States Department of Energy

A Study of Harmonic Distortion Limit Change During the Reconfiguration Process of the Smart Grid

1. Introduction

Over decades, electricity has been commonly used in everybody's daily life because of its convenience, cheapness, and environmental friendliness. The power grid acts like a train that transmits power from the generators to thousands of places where electricity is needed. The electric power grid can be defined as an entirety of machines and transmission lines that connects generators, the source of power, to customers, the users of power [1]. However, the world is experiencing rapid economic development and huge advancements in science, technology and commerce. In the future, the current type of power grid will have difficulties in completing higher requirements in reliability, efficiency and security, as well as the demand of people who pursue higher quality of lives. The current power grid will be replaced gradually (not in the near future) by a new type of power grid named the smart grid, which can accomplish self-healing, wide area monitoring, power flow control, real-time communication (between utility and customers), power quality improvement, and many other important functions.

Self-healing, which includes overload reduction and self-reconfiguration, is one of the most important functions of the smart grid and is considered to be part of its reliability characteristics. For the current power grid, if faults happen at certain locations, it is necessary to manually change the configuration of the system in order to transfer the load connected to the faulted areas to other areas. For other purposes, reconfiguration will be carried out to make the grid operate normally month-by-month or season-by-season depending on electricity usage changes that could be different in different months. The smart grid can accomplish network reconfiguration automatically without human participation based on the data collected by monitors and sensors placed in the system and by feedback data from customers. The smart grid could make the right decisions by resetting the status of certain switches to achieve long-time optimal operation. However, to achieve such an efficient way for the management of the power grid without human action, some of the "traditional customs" might have to be adapted.

Harmonic distortion is a common phenomenon in the power system; it is usually caused by electrical equipment. It could be harmful to a power system in many ways and it is necessary to control it. Left unmanaged, this is a potential pitfall that would undermine the reliability and efficiency of the power system. In the normal case, a distortion limit will be set for the

customer installations by the power provider to limit the maximum distortion they might produce. When reconfiguration is employed to maintain efficiency and reliability of the electric system, the harmonic distortion level of customer installations may change, sometimes dramatically, compared to their original values. The allowable harmonic level produced by a customer load is determined by the customer power demand and short-circuit current (SCC) value at its point of supply. For the current power system, we usually set the distortion limits according to accepted protocols or adopt the “worst case” values for harmonic limits to minimize the harm that the system could experience due to the customer installations. However, when the smart grid concept is applied in operation, new issues are introduced which may affect the present method for setting distortion limits. According to IEEE 519-1992, harmonic distortion limits are determined and classified into several different levels depending on the different sizes of the connected customers. The limits are delimited based on the ratio of short circuit capacity at the customer point of common coupling (PCC) to the maximum load current at the same bus (I_{sc}/I_L). Larger customers will be assigned a larger harmonic distortion limit because they represent a larger portion of the system load [2]. The harmonic distortion limit depends partially on the SCC at the customer PCC, so if the SCC changes with the power system configuration, the harmonic distortion limit sometimes may vary after a smart grid

self-reconfiguration completes. This could make the determination method of the customer harmonic limit different for power providers after the smart grid concept is widely applied in the future.

This thesis will focus on verifying whether appreciable changes in distortion limits will occur at the load buses of a power system before and after reconfiguration. This work will find the harmonic distortion limit after self-reconfiguration at each bus in a test power system and analyze the ranges obtained. If large differences appear at some of the buses, the possibility of harmonic distortion level changes after reconfiguration will be demonstrated and as a result, this phenomenon may be an issue of concern in the smart grid concept. The background of the smart grid concept, the concept of self-reconfiguration, and the importance of the SCC calculation to harmonic distortion limits are introduced in the first chapter. The second chapter consists of a literature review including the history, function and projected impact of the smart grid concept and a detailed introduction and study of reconfiguration in power systems. Definitions, production, and effects of harmonic distortion are considered along with some harmonic studies in smart grids. In the third chapter, the methodology used in this research, including research objectives, the research system (a 30-bus IEEE test power system), the data acquiring tool, and a procedure summary will be presented. The detailed process of

research, including how the original data is converted into per-unit, how the SCC values are obtained in the test system, how harmonic current limits are decided, and the results obtained will be presented in chapter four. The analysis and implication of the results will be present in the final chapter.

2. Literature Review

2.1 An Overview of the Smart Grid – Definition, History, Function, and Future

The power grid in North America is called “the biggest machine in the world.” Hundreds of thousands of customers’ electricity needs are supported by this huge “machine.” However, while its scale is getting larger and larger, power outages happened more frequently year-by-year. As Massoud Amin said, the power outage data from the North American Electric Reliability Council shows that, during the year 2001-2005, outages occurred 140 times at loads whose sizes are over 100 MW, which is much greater than the 76 times during the years 1996-2000, and the 66 times during 1991-1995 for the same load sizes [1]. This data indicates that with the rapid growth of technology and the economy, the current power grid is becoming less capable of preventing power outages. The consideration of a new type of power grid, which is called “smart grid,” was proposed to update the current power grid. The definition of a smart grid can be expressed as a power grid that combines sensing, monitoring, automation and information technology to monitor and control the power system, making it more secure, reliable, efficient, sustainable, and economical [3]. At this time, full functionality is only a concept.

A smart grid can be created by adding smart devices on the normal power grid such as metering, distribution feeders, substations, transmission, and

generation. Devices like sensors and monitors will accomplish the smart metering function. These devices will record the energy usage information in the power system as well as provide two-way communication between power providers and customers. Smart distribution feeders will optimize the operation of the distribution system and offer self-healing, an important function of the smart grid. Furthermore, the complicated structure and operating principles of power distribution will become visible on a computer. The smart substation uses intelligent electric devices inside the substation to optimize the equipment and its operation. Precise power grid control and monitoring is accomplished by smart transmission technology to make transmission lines more effective at delivering energy. New tools are used in smart generation to keep the generation facilities robust, reliable, and efficient, no matter how they are distributed [4].

The goals of developing the smart grid are to realize higher reliability, efficiency，and security by implementing new technologies and to integrate new smart appliances into end use applications. By doing so, the smart appliances can be seen and used in our daily lives. Some effects the smart gird can ultimately offer are [4] [5]:

- A self-healing feature which enables a smart grid to automatically find faults caused by operation mistakes or natural disasters and remove

them in the least amount of time, thus shortening the associated time and cost of locating and removing faults manually in the current power grid; the impact of the faults on end users may also be reduced.

- Resilience against attack by improving the physical integrity of the grid and the protection methods implemented by the smart grid.

- Improvement in power quality from the generation side all the way to customers by minimizing voltage sags and other disturbances.

- Integration of new resources such as solar, wind and geothermal power into the grid to make electricity generation more environmentally friendly.

- Integration of distributed energy storage, plug-in hybrid electric vehicles, and new types of household electric appliances into the power system.

- Improvement of asset utilization efficiency by good planning and precise operation achieved by the processors placed in the system.

- Improved interactions between the grid and customers by providing different plans to them according to their preferences, market needs, and demand response.

- Provide convenience for customers to manage their power usage efficiently according to their patterns of activities by adding advanced metering infrastructure (AMI) and home energy management systems (HEMS).

Driven by potential benefits and profits, the United States implemented a series of policies to support and promote smart grid projects. In 1988, the Electric Power Research Institute (EPRI), which started the study of “Complex Interactive Networks/System Initiative” (CIN/SI), first proposed the concept of the smart grid. In 2001, EPRI promoted the research of “IntelliGrid,” focused on studying its information and communication architecture and on investigating technologies related to the power distribution side. In 2003, the United States Department of Energy (US DoE) published “Grid 2030,” a scheme for the future development of the smart grid. In 2007, the U.S. Congress passed the Energy Independence and Security Act, indicating the importance of the smart grid in legal form. In 2009, President Barack Obama announced that the smart grid would be a focal point in improving the energy industry, increasing job opportunities, and promoting the economy. In February 2009, the American Recovery and Reinvestment Act was initiated and signed by President Barack Obama. This Act specified that 4.5 billion dollars would be invested in

several projects related to developing the smart grid concept. In July 2009, the Federal Energy Regulatory Commission (FERC) issued a final rule, policy statement, and action plan for standards governing the development of a smart grid and offered conclusions about challenges in developing the smart grid in technical, financial, and commercial areas [6] [7] [8].

Though many advantages can be brought by the smart grid concept once fully realized, difficulties still exist and some of them have become the biggest obstacles to implementing it. The smart grid is controlled mainly by computers to which the Internet will be connected, making it vulnerable to attacking means. Once the computers are compromised, the whole power system might fall into disorder and huge losses could occur. Another challenge for smart grid implementation will be the difficulty to manage distributed new resources that may be located far from the loads, making transmission expensive and vulnerable to natural disasters, not to mention the difficulties in forecasting and dispatching power resources that cannot be produced consistently, such as wind power. The privacy of customers is another area to consider: when customer demand responses are received and memorized by the processors of the smart grid, some of their information may need to be shared. As a result, privacy protection will become an important issue with the smart grid [9]. In addition, a lot of new elements and management methods are needed in the smart grid and an

efficient management strategy should be developed in the future so the smart grid as a whole operates well [10]. Lastly, the disturbances (harmonics, etc.) produced by the customer loads during smart grid self-reconfiguration will change in unpredictable ways. Managing customer disturbance emissions will be considered further in Chapters 3 and 4.

2.2 Self-Reconfiguration – An Important Function of the Smart Grid

Network reconfiguration is a common operation that changes the power grid structure by opening and closing ties and switches in a power system when a fault occurs in certain places [11]. In the distribution system, many closed switches and open switches exist, and operators will reconfigure the distribution network by changing the status of some switches regularly (usually by month or season) to fulfill load balancing, eliminate overload, improve power quality, and reduce power losses. When network failure (a short-circuit fault for example) happens, some of the closed switches would be opened to isolate the faulted branch, preventing damage to the whole system. At the same time, some open switches would be closed in order to transfer part of the load from the faulted branch to other branches. As a result, reconfiguration is an important method in improving security, economy, and reliability of the distribution system.

Self-healing, in which self-reconfiguration plays an important part, is a key

feature and has a high significance in the operation of the smart grid. A useful technology in self-healing is fault location, isolation, and service restoration (FLISR), which manages the faults automatically without human involvement in an order such as: detection of the fault through sensors and monitors (fault location), location of the switches on both ends of the fault, isolation of the location at which the fault happened by opening the switches located earlier (isolation), and reconfiguration of the network to connect the loads with backup power resources (service restoration) [4] [12]. This whole process depends on the self-reconfiguration function of the smart grid and can restore power service in about a minute, much faster than the conventional solution of operating manually which requires a long power service suspension for the customers connected to the faulted feeder sections and large amounts of time and money detecting, locating, and restoring the faulted feeder sections [13].

In addition to self-healing, a function called optimal configuration is also associated with the automatic configuration of the smart grid in order to accomplish load balancing. At a specific time, a group of feeders may have peak demands, for example a residential area during 8-10 pm, while another group of feeders may have their peak demands in a different time period, such as an industrial area during work time. Optimal configuration can insure service by the reconfiguration of the network structure to share

the demand between multiple sources, leaving some capacity for better asset utilization [4]. Optimal configuration would also be applied to intentional islanding, which is a method used with special loads that preform better with higher power quality. In this situation, a group of feeders or loads is intentionally isolated from other feeders in the power system, ensuring the best power quality for them [4].

Self-reconfiguration plays an important role in improving the reliability of the smart grid as well as ensuring higher efficiency. However, problems may still exist to prevent the reconfigured system from reaching the best performance. For example, harmonic distortion levels could change dramatically from one configuration to the next. This particular situation is the main focus in this thesis work and is considered in the next section.

2.3 The Causes, Effects, and Solutions for Harmonic Distortion

Harmonics are defined by IEEE 519-1992 as “sinusoidal components of a periodic wave or quantity having frequencies that are integral multiples of the fundamental frequency” [2]. Rectifiers and arc-furnaces, which have nonlinear characteristics while driven by sinusoidal sources, are the most common harmonic injecting devices [14]. Harmonics would bring disturbances, harmonic currents or voltages, which are together called harmonic emissions, to the power system. Harmonic emissions could

cause losses in transmission lines, eddy currents in magnetic devices, and excess heat [15]. The currents and voltages have frequencies that are multiples of the fundamental frequency, which in North America is 60Hz, distorting the original waveform from sinusoidal [16]. When a harmonic current is added to the fundamental current, a non-sinusoidal current waveform will be produced from a sinusoidal voltage waveform produced by a generator, resulting in poor effects that may lower the system efficiency or cause malfunction of some devices [14].

Harmonic currents will produce a magnetic field surrounding the nearby power conductors and devices, possibly inducing current that would have effects on them. Harmonic losses must be added to the amount of heating and sometimes cause equipment de-ratings, the amount of which depends on the frequencies and magnitudes of the harmonic currents. In addition, harmonics could cause malfunction of solid-state devices, the operation of which mainly depends on sensing peak voltage values. The peak voltage values will be disturbed by the presence of harmonics [14].

Harmonic distortion is assessed by total harmonic distortion (THD), defined by IEEE 519 as “total harmonic voltage distortion in percent of nominal

such as IEEE 519, IEC 61000-3-6, and EN 50160, which are adopted differently in different areas of the world [16]. Apart from assessing and regulating harmonics, solutions to minimize them are proposed, and can be summarized mainly to require the adoption of filters. However, measurements to assess harmonic levels will be taken only when some prerequisites are known such as harmonic location and capacitor bank location. These and other particulars are hard to find out in modern complex power systems. As a result, new methods using computer programs are put to use, making harmonic minimization much easier.

2.4 Harmonic Research Related to the Smart Grid

Harmonic distortion creates energy losses, produces excess heat in electric devices and decreases the total efficiency of a power system. This will continue to be a factor reducing the reliability and efficiency of the smart grid which integrates many more electric elements that may produce or be affected by harmonics than the normal power grid. Driven by the novel technology and diverse functions that the smart grid can achieve, more converters will be used for different purposes, from which large amounts of harmonics could be produced. The electronics technology adopted in the converters would increase the switching frequency significantly of the electric switches. Higher switching frequencies decrease the harmonic emissions in the frequency range 0-2.5kHz but

increase the harmonic emission levels at higher frequencies [17]. A greater diversity of loads will also be connected to the smart grid than the normal power grid, bringing more and greater types of harmonic sources. A. Lipsky, N. Miteva, and E. Lokshin did research [18] on one of the consequences caused by harmonics in the smart grid, the commercial loss, which is the active power losses in the transformers that support the harmonic producing installations. The commercial loss is different from technical loss, which is caused by power transmission and distribution. It is the difference between the provided power and received power to a customer [19] and should be counted when calculating the electrical energy balance between the produced and used power. Besides, harmonic distortion has been studied in a lot of research ranging from searching for better ways of measurement to finding new mitigation methods.

In [17], J. Luszcz and R. Smolenski presented the results of voltage harmonic transfer accuracy analyses of voltage transformers in a smart grid. In [15], the researchers worked on the adaptive comb filter, instead of the ones that are conventionally adopted such as FFT and FIR filters, to measure the amplitude of voltage distortion. Works have also been carried out on mitigating harmonics, for example [20] works on improving power quality by mitigating harmonics in a situation where a lot of smart appliances are connected with the smart grid. Because the smart

appliances are nonlinear, active and hybrid filters are considered to be used for mitigation. However, the authors considered the method of using optimal placement of shunt capacitors and rescheduling of load tap changing transformers as the prime methods of mitigation. If the system is highly penetrated by smart appliances, passive capacitor banks were considered to be present at the worst buses, and switching devices were to be rescheduled [20]. Another method presented in [21], which will be different with different methods of using capacitors and rescheduling switching devices, considers harmonic distortion as a part of load management of the smart grid. In normal situations, harmonics are controlled under rated values. Once the harmonic distortion rises to an unacceptable level, it will be detected by applying a harmonic load flow algorithm and controlled by curtailment of excessive loads and reconfiguration of the feeders. The transformer derating value, which is determined by the K-Factor in this paper, will be used to judge whether the harmonic distortion level is beyond a certain limit. Derating is an intentional decrease of transformer load capacity when operating under harmonic distortion. The reason it is adopted is that harmonics cause excess heat that may result in operation beyond rated temperature in the transformer which may lead to failure or loss of life. The authors proposed that when the K-Factor is found to exceed a certain limit, the devices producing the most harmonics would be turned off by smart load management (SLG) and

the users would be notified to change the status of their appliances [21].

The methods of measuring and mitigating harmonics are presented in a lot of papers. However, the changes of harmonic limits during reconfiguration, which will happen frequently in the smart grid, have not been mentioned. In the next chapter, a study will be presented for a 30-bus test system to calculate the harmonic limit changes during the smart grid self-reconfiguration process.

3. Methodology

3.1 Research Target

Improving reliability is a significant objective when designing and constructing a smart grid. One of the important functions that increases the smart grid reliability is self-reconfiguration, through which load balancing, fault detection and power restoration could be completed without human involvement. Harmonic distortion may cause increases in losses and extra heat in electrical devices in the power transmission processes [18]. As a result, assigning harmonic limits to each load of the power system will be important for minimizing the impact of harmonics. However, after self-reconfiguration of the smart grid, the allowable harmonic distortion level of a particular load might change, sometimes dramatically, compared to the original assigned limit, making harmonic limits hard to determine for customer loads. In a normal power grid, the “worst case” limit, which usually is conservative and wasteful, might be used to ensure that none of loads will have their harmonic levels beyond the limits. But in a smart grid, efficiency is also considered to be a prime objective; adoption of the “worst case” assumptions might need to be reconsidered. The purpose of this thesis is to study whether the smart grid self-reconfiguration process affects the harmonic distortion limit values of customer installations set by power providers. If it does, the harmonic distortion limit range will be calculated and the severity level of the effect will be evaluated at each load

bus. Only the load buses will be considered because the limits are used to determine if customer loads can be connected to the power system. As a result, harmonic distortion limit values of sources are excluded from this work.

3.2 Research Design

The study approach will be presented as follows. The harmonic limit ranges will be assessed by calculating both the minimum and the maximum harmonic distortion limits for all the buses. At first, the three-phase symmetrical SCC will be calculated at each load bus when the system operates normally. Secondly, assuming that a fault happens at one branch, making the smart grid automatically change the status of certain switches to remove this branch from the system, the SCC values at every load bus will be calculated again. Thirdly, the initial state of the power system will be restored, which means the branch that was removed in the previous step will be put back. Then, another branch will be removed as the faulted branch, the second step will be repeated, and this process will continue until all the branches have been processed and the results collected. A form will be made using the data obtained including a minimum and a maximum SCC value from each bus. Fourthly, at each load bus, the maximum load current will be calculated and used together with the SCC values to calculate the short circuit ratio, from which we can

find the applicable harmonic current limits at each load bus according to IEEE 519-1992. Fifthly, the buses that show an apparent difference between their minimum and maximum values will be recorded. If those buses exist, the hypothesis will be supported. If they do not exist, the hypothesis fails and a different conclusion will be drawn.

The design of this research is reasonable because when self-reconfiguration is completed, some feeders are connected while others are removed. The design in this work simulates the simplest situation where only one branch will be removed at a time. If harmonic distortion limits change dramatically at some load buses in this simplest situation, it is possible for us to assume that under more complicated scenarios, in which tens of branches could be removed at the same time in a much more complicated power grid, the harmonic distortion limit values would also have great changes. However, under the test system adopted, because it is not a real power system operated in the actuality, the only thing the results would suggest is the possibility that the same situation might happen in a real power system.

In order to complete this study, a 30-bus power system, which is selected from the University of Washington Electrical Engineering website [22], will be used as the study system. The one-line diagram of the system is shown

in Figure 3.1.

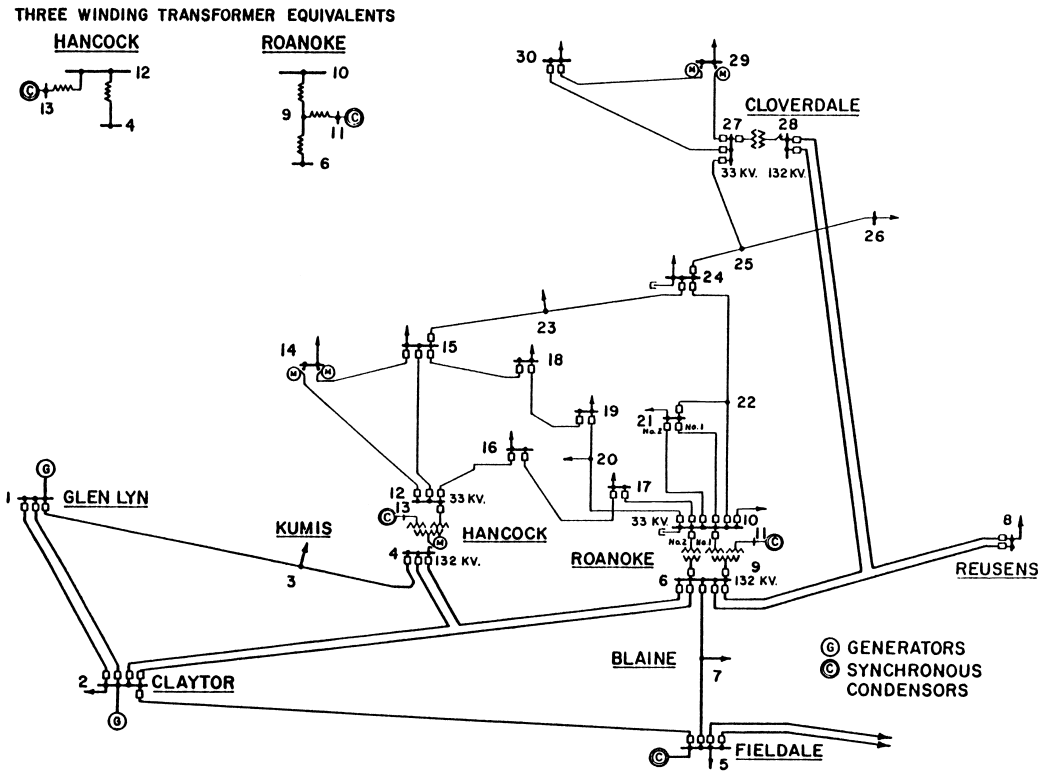

Figure 3.1. The Test Power System

There are 30 buses and 41 branches in this power system and there are 2 generators connected at bus 1 and bus 2 respectively. Twenty-one loads, 2 transformers, and 5 synchronous condensers are also in the system. The bus data are shown in Table 3.1.

BUS#	Voltage Base (KV)	Load (MW)	Load (MVA)	Generation (MW)	Generation (MVAR)	Maximum MVAR
1	132	0.0	0.0	260.2	-16.1	0.0
2	132	21.7	12.7	40.0	50.0	50.0
3	132	2.4	1.2	0.0	0.0	0.0
4	132	7.6	1.6	0.0	0.0	0.0
5	132	94.2	19.0	0.0	37.0	40.0
6	132	0.0	0.0	0.0	0.0	0.0
7	132	22.8	10.9	0.0	0.0	0.0
8	132	30.0	30.0	0.0	37.3	40.0
9	1	0.0	0.0	0.0	0.0	0.0
10	33	5.8	2.0	0.0	0.0	0.0
11	33	0.0	0.0	0.0	16.2	24.0
12	33	11.2	7.5	0.0	0.0	0.0
13	33	0.0	0.0	0.0	10.6	24.0
14	33	6.2	1.6	0.0	0.0	0.0
15	33	8.2	2.5	0.0	0.0	0.0
16	33	3.5	1.8	0.0	0.0	0.0
17	33	9.0	5.8	0.0	0.0	0.0
18	33	3.2	0.9	0.0	0.0	0.0
19	33	9.5	3.4	0.0	0.0	0.0
20	33	2.2	0.7	0.0	0.0	0.0
21	33	17.5	11.2	0.0	0.0	0.0
22	33	0.0	0.0	0.0	0.0	0.0
23	33	3.2	1.6	0.0	0.0	0.0
24	33	8.7	6.7	0.0	0.0	0.0
25	33	0.0	0.0	0.0	0.0	0.0
26	33	3.5	2.3	0.0	0.0	0.0
27	33	0.0	0.0	0.0	0.0	0.0
28	132	0.0	0.0	0.0	0.0	0.0
29	33	2.4	0.9	0.0	0.0	0.0
30	33	10.6	1.9	0.0	0.0	0.0

Table 3.1. The Bus Data of the 30-bus System

The load and generation values are real numbers, which will be converted to per-unit. The sub-transient impedances of the generators and synchronous condensers are not given in Table 3.1, nor are their original power bases. This will be discussed in Chapter 4 along with a way to define their power bases and impedances, as well as how to put them into use in the SCC calculation. The branch data of the system, which contain the impedances of each branch, are shown in Table 3.2. All the per-unit numbers are assumed to be calculated using a power base of 100 MVA and the results are listed in Table 3.1 for the different buses.

Branch #	Resistance (pu)	Reactance (pu)
1,2	0.0192	0.0575
1,3	0.0452	0.1652
2,4	0.0570	0.1737
2,5	0.0472	0.1983
2,6	0.0581	0.1763
3,4	0.0132	0.0379
4,6	0.0119	0.0414
4,12	0.0000	0.2560
5,7	0.0460	0.1160
6,7	0.0267	0.0820
6,8	0.0120	0.0420
6,9	0.0000	0.2080
6,10	0.0000	0.5560
6,28	0.0169	0.0599
8,28	0.0636	0.2000
9,10	0.0000	0.1100
9,11	0.0000	0.2080
10,17	0.0324	0.0845
10,20	0.0936	0.2090
10,21	0.0348	0.0749
10,22	0.0727	0.1499
12,13	0.0000	0.1400
12,14	0.1231	0.2559
12,15	0.0662	0.1304
12,16	0.0945	0.1987
14,15	0.2210	0.1997
15,18	0.1073	0.2185
15,23	0.1000	0.2020
16,17	0.0524	0.1923
18,19	0.0639	0.1292
19,20	0.0340	0.0680
21,22	0.0116	0.0236
22,24	0.1150	0.1790
23,24	0.1320	0.2700
24,25	0.1885	0.3292
25,26	0.2544	0.3800
25,27	0.1093	0.2087
27,28	0.0000	0.3960
27,29	0.2198	0.4153
27,30	0.3202	0.6027
29,30	0.2399	0.4533

Table 3.2. The Branch Data of the 30-bus System

3.3 Analysis Tool

The key to determine a harmonic distortion limit at a bus is the three-phase symmetrical SCC value, which will be obtained by MATLAB in this work. Using the SCC value at all buses, the limits can be developed following the procedures in IEEE 519-1992.

MATLAB is a high-level language and interactive environment for numerical computation, visualization, and programming [23]. It is much easier to write MATLAB codes than other programming tools because it is based on matrices. MATLAB has been widely used in different countries and different professional areas (e.g. numerical analysis, control system simulation, image processing, signal processing, and communication). In electrical engineering, MATLAB is usually used to carry out power flow analyses, control system simulations, result visualizations, etc. In this work, MATLAB will be used to calculate the SCC values at each load bus when a fault happens. System admittance matrices will be built, LDU matrix decompositions and other matrix transformations will be presented, and SCC current values will be calculated.

4 Data Collection Procedure

In order to evaluate the way that the smart grid self-reconfiguration process affects harmonic distortion limits of customer installations, two kinds of data will be collected: both the SCC values before and after self-reconfiguration at all load buses and the maximum load current values for all loads. Based on them, the short-circuit ratio (SCR) can be developed and harmonic distortion limits at each load can be determined from IEEE 519-1992. Through the difference between the original harmonic distortion limits and the new ones, the effect of self-reconfiguration on the smart grid can be clearly revealed. The detailed approach of the analysis will be presented, acquired data will be listed, and a brief summary will be drawn in this chapter.

4.1 The SCC Value Calculation Procedure

The SCC calculation is based on the data presented in Tables 3.1 and 3.2. However, some of the necessary data, such as sub-transient impedances and the manufacturer's power bases of generators and synchronous condensers, are not provided. They will be defined and converted into per-unit in section 4.1.1 using the system power base (100 MVA). In the next two sections, the admittance matrix of the system will be formed using all the data obtained and the theoretical basis of the MATLAB code for the SCC calculation will be explained in detail. In section 4.1.4, the SCC

values (acquired for faults at every load bus for every branch outage) will be listed.

4.1.1 Assignment of the Missing Data

There are two generators connected at buses 1 and 2 and five synchronous condensers connected at buses 2, 5, 8, 11, and 13. The sub-transient impedance used for both generators and synchronous condensers in this work will be assumed to be $X_d'' = 20\%$. Power bases for generator buses will be assigned values which are a conservatively larger than the generator power values; synchronous condenser power bases will be similarly defined as values larger than the maximum reactive powers at each bus given in Table 3.1. For example, the power base at bus 2 will be chosen as 70 MVA, slightly larger than 50 Mvar, which is the value of generated reactive power. All the assigned manufacturer's power bases for generators and synchronous condensers are listed in Table 4.1.

bus #	maximum Mvar	Power Base (MVA)
1	0	270
2	50	70
5	40	45
8	40	45
11	24	30
13	24	30

Table 4.1. Bases for Generators and Synchronous Condensers

Sub-transient impedances will be assigned after power bases. With per-unit data $X_d'' = 20\%$ assumed, the first step is to transform a per-unit

equation

$$X_{real} = X_d'' \cdot \frac{V_{base}^2}{S_{base-manu}} \quad (4.1)$$

where

X_{real} = real sub-transient reactance of generators and synchronous condensers in SI units,

V_{base} = nominal line-to-line voltages at each related bus, and

$S_{base-manu}$ = manufacturer's three-phase power bases of generators and synchronous condensers.

The second step is to transform the real values back into per-unit values using the system power base of 100 MVA (provided in the original system information) and the equation

$$X_{pu} = X_{real} \cdot \frac{S_{baes-sys}}{V_{base}^2} \quad (4.2)$$

where

X_{pu} = per-unit reactance values of generators and synchronous condensers using 100 MVA power base and

$S_{base-sys}$ = 100 MVA.

The calculated per-unit reactance values of generators and synchronous condensers are listed in Table 4.2. The resistances of all sources will be neglected.

Bus #	equipment type	reactance in per-unit
1	generator	0.074
2	generator	0.285
2	condenser	0.285
5	condenser	0.44
8	condenser	0.44
11	condenser	0.67
13	condenser	0.67

Table 4.2. Per-unit Reactance Values for Generators and Synchronous Condensers

4.1.2 The Method Used for Calculating the Three-Phase SCC [24]

Suppose a short-circuit fault happens at the node f through an impedance z_f, which will not be a part of the system admittance matrix, as shown in Figure 4.1.

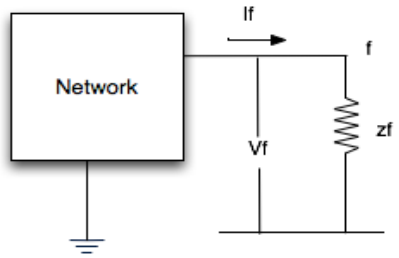

Fig 4.1. Short-Circuit Analysis

If we separate the faulted branch from the original network, which as a whole can be considered unchangeable but only encountering an injection current $-I_f$, making the voltage at any node i expressed as

$$V_i = \sum_{j \in G} (Z_{ij} \cdot I_j) - Z_{if} \cdot I_f \tag{4.3}$$

where

$Z_{ij} =$ impedance between node i and node j,

$Z_{if} =$ impedance between node i and the fault node f,

$I_j =$ current flow into node j, and

the letter G represents all nodes in the network.

The first part $\sum_{j \in G} (Z_{ij} \cdot I_j)$ represents the voltage at node i generated by the sources in the system before the short-circuit fault happens at node f and is used in a simplified notation as

$$V_i^{(0)} = \sum_{j \in G} (Z_{ij} \cdot I_j). \quad (4.4)$$

The second part $-Z_{if} \cdot I_f$ represents the voltage, which may be called the fault component, generated by the SCC I_f at node i. As a result, (4.3) can be expressed as

$$V_i = V_i^{(0)} - Z_{if} \cdot I_f. \quad (4.5)$$

Equation 4.5 also works for node f, so replacing i with f gives

$$V_f = V_f^{(0)} - Z_{ff} \cdot I_f \quad (4.6)$$

where

$V_f^{(0)}$ = voltage of fault node f before the short-circuit happens and

Z_{ff} = the impedance that connected to node f.

After (4.6) is developed, another equation shown in (4.7) is still needed because there are two unknowns, V_f and I_f, to be determined.

$$V_f - z_f \cdot I_f = 0 \quad (4.7)$$

In (4.7),

$z_f =$ the fault impedance.

Combining (4.6) and (4.7), the SCC at the node f can be expressed as

$$I_f = {V_f^{(0)}}\Big/{(Z_{ff} + z_f)}. \tag{4.8}$$

It should be noticed that in (4.8), all the elements have the subscript "f," which means the SCC I_f can be calculated using rows and columns related only to "f" in the impedance matrix instead of using the whole matrix when $V_f^{(0)}$ is known. In fact, when a three-phase short-circuit fault happens, the impedance $z_f = 0$, making (4.8) turn into (4.9), which is much simpler to solve.

$$I_f = {V_f^{(0)}}\Big/{Z_{ff}} \tag{4.9}$$

In the short-circuit calculation process, some values can be assumed as known or simply be ignored in the power system, simplifying the calculation procedure. The resistances of generators, transformers, and transmission lines are neglected; all the loads and transmission line capacitances are ignored; during per-unit value calculations, the differences between load rated voltages and bus rated voltages are ignored when identifying the latter as the voltage bases; the transformer ratios are considered as unity in per-unit; and the same voltage potentials are applied to all the generators.

After simplification, (4.9) can be further simplified as shown in (4.10) because all the effects of loads are ignored, making voltages equal to unity

at all load buses.

$$I_f = {}^{1}/_{Z_{ff}} \tag{4.10}$$

As a result, the only element needed to calculate the three-phase SCC would be the impedance Z_{ff} connected with the fault bus. It can be determined from the admittance matrix of the system and its decomposition. The elements that form the admittance matrix are the transmission line reactance values listed in Table 3.2 and the reactances of generators and synchronous condensers shown in Table 4.1.

4.1.3 The Process of Obtaining the Impedance Matrix $[Z]$

Equation 4.10 clearly indicates that the system impedance matrix, which is difficult to obtain directly, is necessary when calculating the SCC. However, by building the system admittance matrix $[Y]$, which is much easier to do, the impedance matrix $[Z]$ can be obtained by inverting $[Y]$ because of their mutually invertible nature

$$\boldsymbol{YZ_j} = \boldsymbol{e_j} \ (j = 1,2,\dots,n) \tag{4.11}$$

where

$\boldsymbol{Z_j}$ = the column vector composed of the column j in the impedance matrix and

$\boldsymbol{e_j}$ = the unity column vector whose j-th element is unity and the other elements are zero.

In fact, elements in (4.11) have actual physical meanings. Define $[e_j]$ as

the column vector of node-injected currents and $[Z_j]$ as the column vector of node voltages. When unit current is injected only into node j and no current appears at the remaining nodes, the values of node voltages will be equal to the values in the j-th column in the impedance matrix [24].

In this 30-bus power system, since all the resistances are ignored, $[Y]$ is a 30×30 matrix with the general entry

$$\overline{y}_{ij} = -jb_{ij} = -j\frac{1}{X_{ij}} \ . \tag{4.12}$$

In the matrix, the element $\overline{y}_k$, connected between nodes i and j, will be added to four basic elements: $\overline{y}_{ii}$, $\overline{y}_{ij}$,$\overline{y}_{ji}$, and $\overline{y}_{jj}$. The general procedure for constructing $[Y]$ can be summarized in (4.13)-(4.16) [25]. The values of elements connected from a bus to reference are assumed to be zero for branches.

$$\overline{y}_{ii_{new}} = \overline{y}_{ii_{old}} + \overline{y}_k \tag{4.13}$$

$$\overline{y}_{jj_{new}} = \overline{y}_{jj_{old}} + \overline{y}_k \tag{4.14}$$

$$\overline{y}_{ij_{new}} = \overline{y}_{ij_{old}} - \overline{y}_k \tag{4.15}$$

$$\overline{y}_{ji_{new}} = \overline{y}_{ji_{old}} - \overline{y}_k \tag{4.16}$$

This method will be used in this work to obtain the admittance matrix because not only does it apply to a 30-bus (relatively complex) system, which is difficult to analyze and calculate manually while easy to program using MATLAB, but also shows its advantage of modifying the admittance matrix if there are branches that need to be removed or added due to

system changes [25].

The admittance matrix $[Y]$ is a nonsingular matrix which can be factorized using the Doolittle Algorithm into three matrices $[L]$, $[D]$, and $[U]$.

$$\boldsymbol{Y = LDU} \tag{4.17}$$

Because triangular matrices $[U]$ and $[L]$ are mutual transpositions of each other, it is appropriate to calculate only one of them, which will be matrix $[U]$ in this thesis. The expressions for the basic factors in $[D]$ and $[U]$ are shown in (4.18) and (4.19)

$$d_{ii} = a_{ii} - \sum_{k=1}^{i-1} u_{ki}^2 d_{kk} \quad (i = 1,2, \dots, n) \tag{4.18}$$

$$u_{ij} = (a_{ij} - \sum_{k=1}^{i-1} u_{ki} u_{kj} d_{kk})/d_{ii} \quad \binom{i=1,2,\dots,n-1}{j=i+1,\dots,n} \tag{4.19}$$

After the factorization of $[Y]$, (4.11) can be written as (4.20) which can be further decomposed into three equations in (4.21).

$$\boldsymbol{LDUZ_j = e_j} \tag{4.20}$$

$$\left.\begin{aligned} \boldsymbol{LF} &= \boldsymbol{e_j} \\ \boldsymbol{DH} &= \boldsymbol{F} \\ \boldsymbol{UZ_j} &= \boldsymbol{H} \end{aligned}\right\} \tag{4.21}$$

The general entries of matrices $[F]$, $[H]$, and $[Z_j]$ are shown in Equation (4.22)-(4.24).

$$f_i = \begin{cases} 0 & i < j \\ 1 & i = j \\ -\sum_{k=j}^{i-1} u_{ki} f_k & i > j \end{cases} \tag{4.22}$$

$$h_i = \begin{cases} 0 & i < j \\ f_i/d_{ii} & i \geq j \end{cases} \tag{4.23}$$

$$Z_{\dots} = \sum^{n} \dots \tag{4.24}$$

By defining the value of j, all the elements shown in the impedance matrix $[Z]$ can be obtained including Z_{ff}, the faulted node's self-impedance, that will be used in (4.10). As a result, the SCC values can be solved at all buses which are assumed to experience short-circuit faults [9].

4.1.4 The Flow Diagram of MATLAB Programming

The methods, which include building the admittance matrix $[Y]$, obtaining the impedance matrix $[Z]$, and a simplified way to calculate the three-phase SCCs, are adopted and implemented in MATLAB. The diagram of the programming process is shown in Figure 4.2.

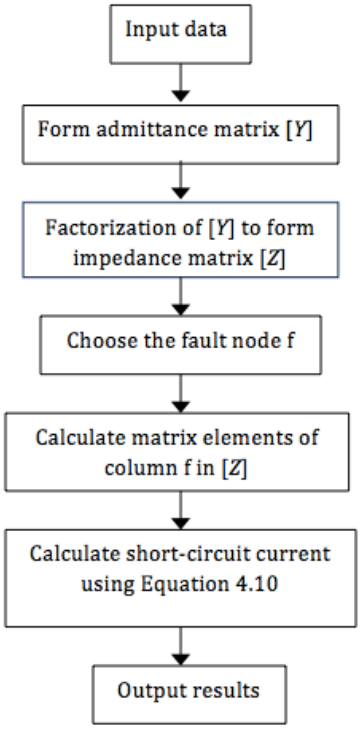

Figure 4.2. Flow Diagram of MATLAB Programming

4.1.5 Results

As discussed in the third chapter, the SCC values will be calculated for faults at every load bus whenever a branch disconnects from the system. Therefore, each load bus will have 41 different SCC values with respect to each of the 41 branches in the power system. For example, at bus 2, a bus which has both a generator and a load, the SCC value will be first calculated when no branch is disconnected, then calculated again when only branch (1,2) is disconnected, and then branch (1,3) and so forth, until the last branch has been considered. Numerous results will be obtained in the process, but only the ones needed (the maximum and minimum SCC values at every load bus) are listed in Table 4.3. These two values are retained due to this chapter's focus, which is on the largest numerical difference between the SCC values at each load bus before and after the smart grid reconfiguration. All the data shown in Table 4.3 are their per-unit absolute values which do not contain the imaginary symbol j.

BUS #	Maximum value	Minimum value
2	14.0108	7.9231
3	10.1656	4.5386
4	12.0640	8.0460
5	8.1397	5.7028
7	8.1284	3.4891
8	9.7334	5.1019
10	5.6639	3.7108
12	5.5941	3.5175
14	3.3669	2.2819
15	4.4115	3.0991
16	3.8637	2.1360
17	4.4327	1.7079
18	3.1805	1.6963
19	3.1948	1.6704
20	3.3742	1.5000
21	4.6721	3.3561
23	3.2320	1.6616
24	3.7000	2.1689
26	1.3207	0.8998
29	1.5301	0.7085
30	1.4059	0.8169

Table 4.3. Maximum and Minimum SCC Per-Unit Values Calculated at All Load Buses

It is worth noting that all of the maximum values in Table 4.3 are acquired in the situation when no branch is disconnected from the system, implying that the SCC values will be largest under normal conditions without any reconfiguration completed by the smart grid. On the other hand, when a disconnected branch exists, the SCC values at all the load buses will decrease, indicating that reconfiguration will affect the SCC values, therefore possibly affecting harmonic distortion limits for customer loads.

4.2 The Maximum Load Current (MLC) Values Acquisition Process

Harmonic distortion limits given in IEEE 519-1992 depend on the ratio of the SCC value at the PCC to the maximum fundamental load current (MLC) value. The MLC values are calculated as the average current values of the maximum demand for the preceding 12 months [2]. In this work, the MLC values will be evaluated using the load data provided in column 3, column 4, and the nominal voltages shown in column 2 in Table 3.1. First, the maximum load power values are calculated using the load's active and reactive power. The equation of the process is shown in (4.25).

$$S_{load} = \sqrt{P_{load}^2 + Q_{load}^2} \tag{4.25}$$

In order to obtain the MLC values in per-unit, the current bases at all load buses should be acquired using (4.26). The three-phase power base is the system base (100 MVA); the variable V_{base} is numerically equal to V_n, the nominal line-to-line voltage.

$$I_{base} = {S_{base}}\Big/{\sqrt{3}V_{base}} \tag{4.26}$$

The results are listed in Table 4.4.

BUS #	Vn (KV)	S_load (MVA)	I_base (A)
2	132	25.14	437.38
3	132	2.68	437.38
4	132	7.77	437.38
5	132	95.90	437.38
7	132	25.27	437.38
8	132	42.43	437.38
10	33	6.14	1749.54
12	33	13.48	1749.54
14	33	6.40	1749.54
15	33	8.57	1749.54
16	33	3.94	1749.54
17	33	10.71	1749.54
18	33	3.32	1749.54
19	33	10.10	1749.54
20	33	2.31	1749.54
21	33	20.78	1749.54
23	33	3.58	1749.54
24	33	10.98	1749.54
26	33	4.19	1749.54
29	33	2.56	1749.54
30	33	10.77	1749.54

Table 4.4. Data Needed to Calculate the Maximum Load Current

The MLC real values in SI units will be determined from the three-phase load power S_{load} and the bus nominal line-to-line voltages V_n as shown in (4.27).

$$I_{load\ real} = {S_{load}}/{\sqrt{3}V_n} \tag{4.27}$$

In the end, the MLC values at all load buses are calculated as shown in (4.28), and the results are displayed in Table 4.5.

$$I_{load\ pu} = {I_{load\ real}}/{I_{base}} \tag{4.28}$$

BUS #	I_load real (A)	I_load pu
2	110.00	0.2515
3	11.74	0.0268
4	33.94	0.0776
5	419.47	0.9591
7	110.53	0.2527
8	185.61	0.4244
10	107.56	0.0615
12	235.73	0.1347
14	112.11	0.0641
15	150.00	0.0857
16	68.78	0.0393
17	187.25	0.1070
18	58.18	0.0332
19	152.41	0.0871
20	40.30	0.0230
21	363.60	0.2078
23	62.72	0.0358
24	192.10	0.1098
26	73.33	0.0419
29	44.84	0.0256
30	188.47	0.1077

Table 4.5. Real and Per-Unit Values of the Maximum Load Current

4.3 Results of Short-Circuit Ratio and Total Demand Distortion

After obtaining the SCC values and the MLC values at all load buses, the short-circuit ratios (SCR) can be found using the latter to divide the former. The total demand distortion (TDD) limits can be found using the SCRs. The TDD is defined by IEEE 519-1992 as harmonic current distortion in percent of the maximum demand current. Data presented in Tables 4.3 and 4.5 will be used to calculate the SCR values using (4.29) and (4.30), the results of which are shown in Table 4.6.

$$SCR_{min} = {I_{sc\ min}}/{I_{load\ pu}} \quad (4.29)$$

$$SCR_{max} = {I_{sc\ max}}/{I_{load\ pu}} \quad (4.30)$$

BUS #	SCR_min	SCR_max
2	32	56
3	169	379
4	104	155
5	6	8
7	14	32
8	12	23
10	60	92
12	26	42
14	36	53
15	36	51
16	54	98
17	16	41
18	51	96
19	19	37
20	65	146
21	16	22
23	46	90
24	20	34
26	21	32
29	28	60
30	8	13

Table 4.6. SCR Values at the PCC of All Load Buses

The TDD limit values can be found in Tables 10.3 and 10.4 in IEEE 519-1992 and are presented in Table 4.7.

BUS #	Vn (KV)	TDD_min (%)	TDD_max (%)	# of increments
2	132	4.0	6.0	1
3	132	7.5	7.5	0
4	132	7.5	7.5	0
5	132	2.5	2.5	0
7	132	2.5	4.0	1
8	132	2.5	4.0	1
10	33	12.0	12.0	0
12	33	8.0	8.0	0
14	33	8.0	12.0	1
15	33	8.0	12.0	1
16	33	12.0	12.0	0
17	33	5.0	8.0	1
18	33	12.0	12.0	0
19	33	5.0	8.0	1
20	33	12.0	15.0	1
21	33	5.0	8.0	1
23	33	8.0	12.0	1
24	33	8.0	8.0	0
26	33	8.0	8.0	0
29	33	8.0	12.0	1
30	33	5.0	5.0	0

Table 4.7. The TDD Limit Values Obtained from IEEE 519-1992

The data listed in Table 4.7 present the fact that although at some buses, for example buses 3, 4, 5, and 18, no difference can be observed between the maximum and minimum values. At some load buses, there are apparent differences between maximum and minimum values, such as buses 2, 14, and 20. The TDD values of most of these changed one increment from 4% to 6%, 8% to 12%, and 12% to 15%. At bus 16 and 18, although no TDD value changes can be observed, their SCR values are very close to the SCR boundary values. For example, at bus 16, the minimum SCR value is 54 which is very close to 50, the minimum boundary value; the maximum SCR value is 98 which is very close to 100,

the maximum boundary value. This means that although in this test system there are no TDD value changes shown at buses 16 and 18, there might be 2 increments in another system because both their minimum and maximum SCR values are very close to the SCR boundary values.

The results reveals that in the test system, the harmonic distortion limits for customer installations will be different after the smart grid self-reconfiguration. At some load buses there are differences. At some other buses, although large differences do not appear, the potential to have a large difference is shown. Although it is not a real system, such results may suggest the possibility that similar changes may also occur in a real power system supporting real customer loads. Considering the negative effects of the harmonics and the reliability and efficiency goals that a smart grid is trying to fulfill, this issue may require people's attention when making the effort to design and develop the smart grid concept. Ignoring this issue may result in undesirable consequences.

4.4 The Study of Patterns in SCR Value Distributions at Different Load Buses

In the 30-bus test system, the SCRs are calculated at each load bus when 41 branches are taken out one-by-one. The SCR values determine directly the harmonic distortion limits assigned to every load bus. However, in

some load buses in the test system, the maximum SCR values shown in Table 4.1 are just a little larger or smaller than the boundary values shown in the first column of the tables in IEEE 519-1992 which are repeated here in Tables 4.8 and 4.9 [2].

Maximum Harmonic Current Distortion in Percent of Maximum Load Current						
Individual Harmonic Order (Odd Harmonics)						
Isc/Il	<11	11<=h<17	17<=h<23	23<=h<35	35<=h	TDD
<20	4.0	2.0	1.5	0.6	0.3	5.0
20<50	7.0	3.5	2.5	1.0	0.5	8.0
50<100	10.0	4.5	4.0	1.5	0.7	12.0
100<1000	12.0	5.5	5.0	2.0	1.0	15.0
>1000	15.0	7.0	6.0	2.5	1.4	20.0

Table 4.8. Current Distortion Limits for General Subtransmission Systems (120 V Through 69000 V)

Maximum Harmonic Current Distortion in Percent of Maximum Load Current						
Individual Harmonic Order (Odd Harmonics)						
Isc/Il	<11	11<=h<17	17<=h<23	23<=h<35	35<=h	TDD
<20	2.0	1.0	0.8	0.3	0.2	2.5
20<50	3.5	1.8	1.3	0.5	0.3	4.0
50<100	5.0	2.3	2.0	0.8	0.4	6.0
100<1000	6.0	2.8	2.5	1.0	0.5	7.5
>1000	7.5	3.5	1.3	0.7	10.0	20.0

Table 4.9. Current Distortion Limits for General Subtransmission Systems (69001 V Through 161000 V)

It is questionable whether the maximum SCR value will always be larger than the boundary value or if it only happens occasionally. In this situation the SCR value might not be effective to determine the harmonic distortion limit from Table 4.8 or Table 4.9. But if this SCR value is larger than the boundary value in most cases, then we can say that the associated harmonic distortion limit could be found using this larger SCR value. As a result, it is helpful if a distribution pattern of the 41 SCR values is considered because it can help to estimate which single value to use for any actual customer limits.

In this work, 5 buses are studied and all of them have the same pattern of value distribution. This pattern can be described as: most SCR values show little difference compared to the maximum SCC value of the same bus.

For bus 2, among the 41 values, 40 of them appear in the range from 50 to 60, with the maximum value being 55.71; for bus 7, 36 values are in the range from 30 to 40, with the maximum value being 32.17; for bus 16, 35 values appear in the range from 90 to 100, with the maximum value being 98.31; for bus 18, 33 values are in the range from 90 to 100, with the maximum value being 95.80; for bus 20, 30 values are in the range from 140 to 150, with the maximum value being 146.70. The SCR value

histograms of bus 2, bus 7, bus 16, bus 18, and bus 20 are shown in Figures 4.3-4.7. The y-axis represents the number of times (out of 41) that an SCR value fell in a certain range; the x-axis represents different SCR value ranges in per-unit. The red lines in the pictures represent the boundary values from the IEEE 51-1992 tables.

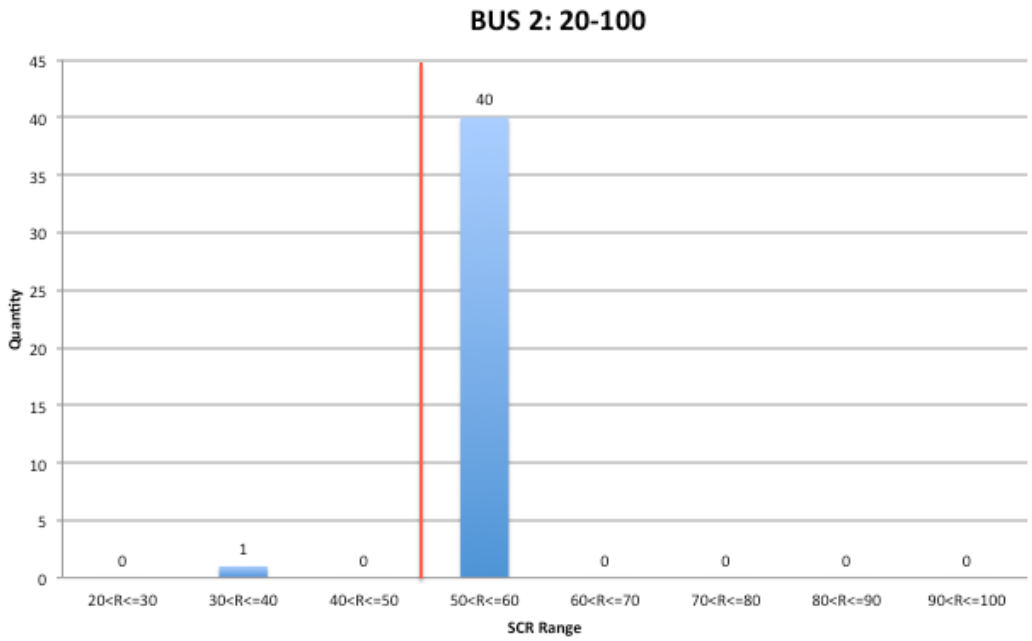

Figure 4.3. Histogram of the SCR Values at Bus 2

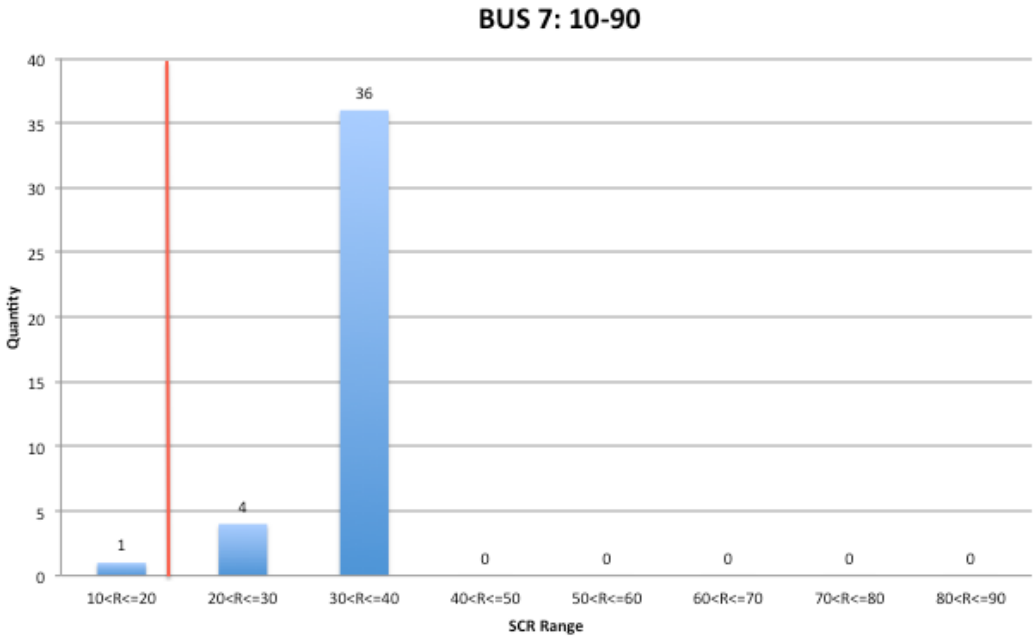

Figure 4.4. Histogram of the SCR Values at Bus 7

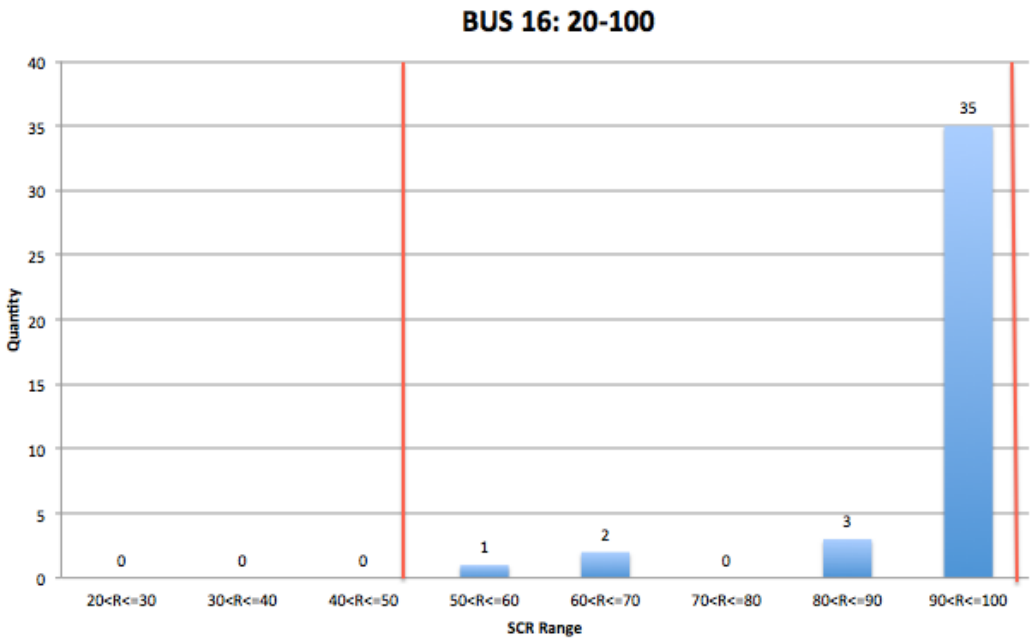

Figure 4.5. Histogram of the SCR Values at Bus 16

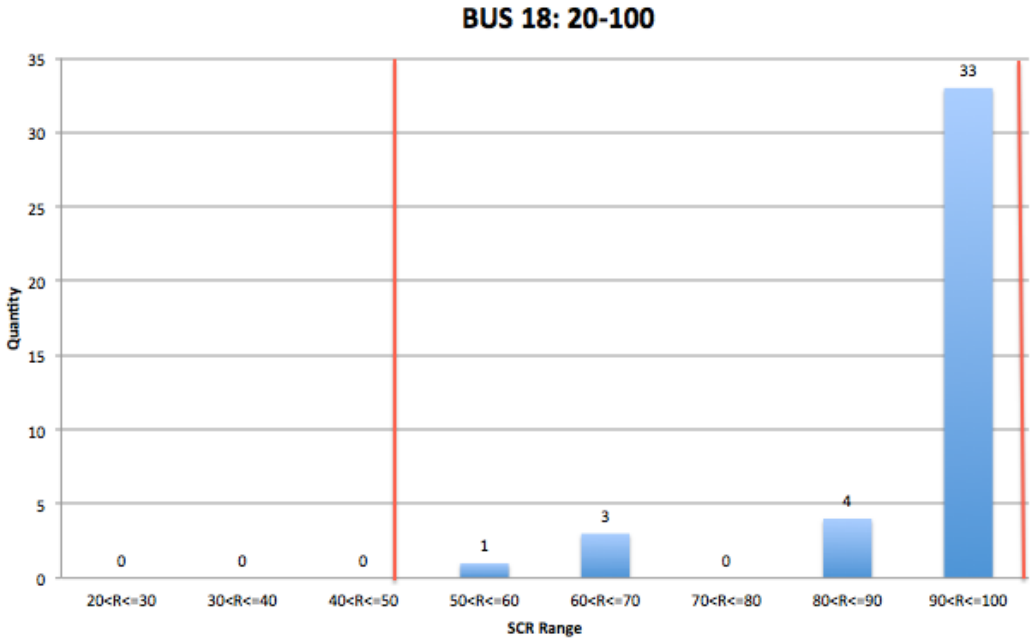

Figure 4.6. Histogram of the SCR Values at Bus 18

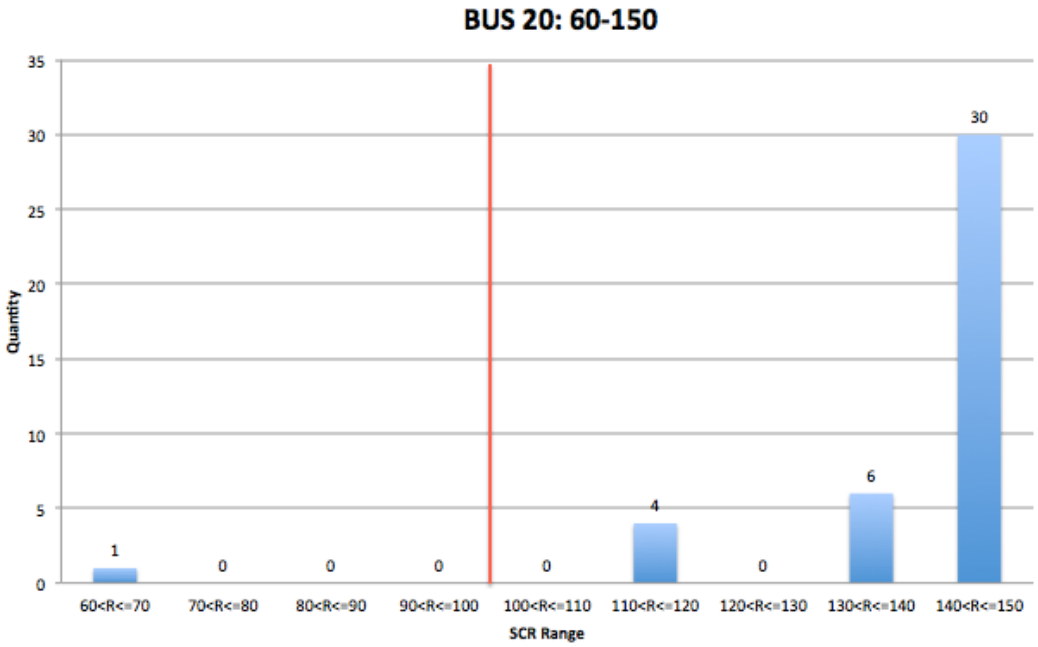

Figure 4.7. Histogram of the SCR Values at Bus 20

From the histograms, we can find that most of the SCR values are close to their maximum values, which suggests that even though some of the maximum values are close to the boundaries, they are reliable bases for harmonic limits.

5. Conclusions and Discussions

In this thesis, the possibility is proposed that the smart grid self-reconfiguration process may change the original harmonic distortion limit values set by the power provider. This hypothesis is tested by designing an experiment with a 30-bus test power system in which the harmonic distortion limit values of some buses changed compared to the original values obtained using maximum short-circuit current, suggesting the possibility of similar or greater changes in other systems.

One of the methods that the smart grid would use to ensure its reliability and efficiency is to reconfigure its structure in order to isolate a faulted branch, restore power, take advantage of distributed power sources, fulfill load balancing, or avoid peak demand hours of certain feeders. However, a hypothesis was made and verified that the harmonic distortion limits that have already been set by power providers might change after the reconfiguration. This change could certainly increase the complexity of smart grid operations.

In order to test the hypothesis, an algorithm was proposed where the process of removing the branches one-by-one from the test system (one branch each time) was used to simulate the most simple smart grid self-reconfiguration process. Harmonic distortion limits after this simulated

reconfiguration process were calculated by obtaining and using the SCC and MLC values at each bus according to the method presented in IEEE 519-1992. The SCC values were obtained by writing a MATLAB code according to the method presented in [24].

The results proved the hypothesis that in the test system, the harmonic distortion limits of some buses would decrease after the self-reconfiguration process compared to their original values. This situation suggests that the possibility exists in a real smart grid that harmonic distortion limits would also change after self-reconfiguration. In this situation, adoption of “worst case” assumptions, which is normally done today, might not be applicable for the smart grid because the “worst case” assumptions may lead to decisions that have negative effects on reliability and efficiency which are the chief goals of the smart grid.

References

[1] M. Amin, “Challenges in Reliability, Security, Efficiency, and Resilience of Energy Infrastructure: Toward Smart Self-healing Electric Power Grid,” IEEE Power and Energy Society General Meeting - Conversion and Delivery of Electrical Energy in the 21st Century, pp. 1-5, 2008.

[2] IEEE Recommended Practices and Requirements for Harmonic Control in Electrical Power Systems, IEEE Standard 519-1992, pp. 1-112, 1993.

[3] Z. Liu, “Smart Grid Technology,” Beijing: China Electric Power Press, 2010 (In Chinese).

[4] R. W. Usulki, “The Role of Advanced Distribution Automation in the Smart Grid,” 2010 IEEE Power and Energy Society General Meeting, pp. 1-5, 2010.

[5] K. Moslehi and R. Kumar, “Smart Grid – a reliability perspective,” Innovative Smart Grid Technologies (ISGT), pp. 1-8, 2010.

[6] “What is the Smart Grid?” Retrieved February 24th, 2014, from http://www.smartgrid.gov/the_smart_grid#smart_grid.

[7] “Smart grid in the United States,” 2013, Retrieved February 24th, 2014, from http://en.wikipedia.org/wiki/Smart_grid_in_the_United_States.

[8] X. Xu, “Smart Grid introduction,” Beijing: China Electric Power Press, 2009 (In Chinese).

[9] F. Beidou, W. Morsi, C. Diduch, and L. Chang, “Smart Grid: Challenges, Research Directions and Possible Solutions,” 2010 2nd IEEE International Symposium on Power Electronics for Distributed Generation Systems (PEDG), pp. 670-673, 2010.

[10] F. Bouhafs, M. Mackay, and M. Merabti, “Links to the Future: Communication Requirements and Challenges in the Smart Grid,” IEEE Power and Energy Magazine, vol. 10, no. 1, 2012.

[11] C. Ababei and R. Kavasseri, “Efficient Network Reconfiguration Using Minimum Cost Maximum Flow-Based Branch Exchanges and Random Walks-Based Loss Estimations,” IEEE Transactions on Power Systems, vol. 26, no.1, pp. 30-37, 2011.

[12] M. Shahin, “Smart Grid self-healing implementation for underground distribution networks,” 2013 IEEE Innovative Smart Grid Technologies

Asia (ISGT Asia), pp. 1-5, 2013.

[13] J. Agüero, “Applying self-healing schemes to modern power distribution system,” IEEE Power and Energy Society General Meeting, pp. 1-4, 2012.

[14] S. Subjak, Jr, J. Mcqilkin, “Harmonics - Causes, Effects, Measurements, and Analysis- An Update,” IEEE transactions on industry applications, vol. 26, no. 6, pp. 1034-1042, 1990.

[15] B. Emayavaramban, R. Shiyagarajan, B. Vivek, Y. S. Kishan, and P. Sapria, “Amplitude Computation of Harmonic Voltages based on Adaptive Comb Filter in a Smart Grid System,” IEEE Conference on Information & Communication Technologies (ICT), pp. 42-46, 2013.

[16] R. Tan, V. Ramachandaramurthy, “Real time power system harmonic distortion assessment virtual instrument,” IEEE 15th international conference on harmonics and quality of power (ICHQP), pp. 791-795, 2012nformation & Communication Technologies (ICT), pp. 42-46, 2013.

[17] J. Luszcz, R. Smolenski, “Voltage Harmonic Distortion Measurement Issue in Smart-Grid Distribution System,” Asia-Pacific Symposium on Electromagnetic Compatibility (APEMC), pp. 841-844, 2012.

[18] A. Lipsky, N. Miteva, and E. Lokshin, “Current harmonics and commercial losses in smart grid,” 2012 3rd IEEE PES International Conference and Exhibition on Innovative Smart Grid Technologies (ISGT Europe), pp. 1-5, 2012.

[19] “Reducing technical and non-technical losses in the power sector,” Background paper of the World Bank group energy sector strategy, July 2009.

[20] M. Masoum, S. Deilami, and S. Islam, “Mitigation of Harmonics in Smart Grids With High Penetration of Plug-In Electric Vehicles,” 2010 IEEE Power and Energy Society General Meeting, pp. 1-6, 2010.

[21] M. Masoum, P. Moses, S. Deilami, “Load Management in Smart Grids Considering Harmonic Distortion and Transformer Derating,” 2010 Innovative Smart Grid Technologies (ISGT), pp. 1-7, 2010.

[22] R. Christie, “Power Systems Test Case Archive,” August 1993, Retrieved February 17th, 2014, from http://www.ee.washington.edu/research/pstca/pf30/pg_tca30bus.htm.

[23] “MATLAB: The Language of Technical Computing,” Retrieved February 18th, from http://www.mathworks.com/products/matlab/.

[24] Y. He and Z. Wen, “Power System Analysis,” Wuhan: Huazhong University of Science and Technology press, January 1st, 2002, pp. 1-268.

[25]. C. Gross, “Power System Analysis,” New York: John Wiley & Sons, 1986.